



LAWRENCE  
LIVERMORE  
NATIONAL  
LABORATORY

# The Role of a Detailed Configuration Accounting (DCA) Atomic Physics Package in Explaining the Energy Balance in Ignition Scale Hohlräume

M. Rosen, H. Scott, D. Hinkel, E. Williams, D. Callahan, R. Town, L. Divol, P. Michel, W. Kruer, L. Suter, R. London, J. Harte, G. Zimmerman

January 12, 2011

High Energy Density Physics

## **Disclaimer**

---

This document was prepared as an account of work sponsored by an agency of the United States government. Neither the United States government nor Lawrence Livermore National Security, LLC, nor any of their employees makes any warranty, expressed or implied, or assumes any legal liability or responsibility for the accuracy, completeness, or usefulness of any information, apparatus, product, or process disclosed, or represents that its use would not infringe privately owned rights. Reference herein to any specific commercial product, process, or service by trade name, trademark, manufacturer, or otherwise does not necessarily constitute or imply its endorsement, recommendation, or favoring by the United States government or Lawrence Livermore National Security, LLC. The views and opinions of authors expressed herein do not necessarily state or reflect those of the United States government or Lawrence Livermore National Security, LLC, and shall not be used for advertising or product endorsement purposes.

**The Role of a Detailed Configuration Accounting (DCA)  
Atomic Physics Package in Explaining the Energy Balance in  
Ignition Scale Hohltraums**

M. D. Rosen\*, H. A. Scott, D. E. Hinkel, E. A. Williams, D. A. Callahan, R. P. J. Town,  
L. Divol, P. A. Michel, W. L. Kruer, L. J. Suter, R. A. London, J. A. Harte, and G. B.  
Zimmerman

Lawrence Livermore National Laboratory  
7000 East Avenue, P. O. Box 808  
Livermore, CA 94551-0808 USA

**Abstract**

In 2009 the National Ignition Campaign (NIC) gas filled/capsule imploding hohlraum energetics campaign showed good laser-hohlraum coupling, reasonably high drive, and implosion symmetry control via cross beam transfer. There were, however, discrepancies with expectations from the standard simulation model including: the level and spectrum of the Stimulated Raman light; the tendency towards pancake-shaped implosions; and drive that exceeded predictions early in the campaign, and lagged those predictions late in the campaign. We review here the origins / development path of the “high flux model” (HFM). The HFM contains two principal changes from the standard model: 1) It uses a detailed configuration accounting (DCA) atomic physics non-local-thermodynamic-

equilibrium (NLTE) model, and 2) It uses a generous electron thermal flux limiter,  $f=0.15$ , that is consistent with a non-local electron transport model. Both elements make important contributions to the HFM's prediction of a hohlraum plasma that is cooler than that predicted by the standard, NLTE average atom,  $f=0.05$  model. This cooler plasma is key in eliminating most of the discrepancies between the NIC data and revised expectations now based on this new simulation model. The HFM had previously been successfully deployed in correctly modeling Omega Laser illuminated gold sphere x-ray emission data, and NIC empty hohlraum drive. However, when the HFM was first applied to this energetics campaign, the model lacked some credibility / acceptance because, compared to the standard model, it actually worsened the discrepancy between the observed hohlraum drive (for the 1 MJ class experiments performed late in the campaign) and the revised expectation of higher drive based on the HFM. Essentially, the HFM was making a prediction that the laser-hohlraum coupling was less than that assumed at that time. Its credibility was then boosted when a re-evaluation of the losses matched its prediction.

\*Corresponding author

L-039, LLNL, Livermore, CA 94551, [rosen2@llnl.gov](mailto:rosen2@llnl.gov), (925) 422-5427

PACS #s: 52.25.Os, 52.38.Ph, 52.57.Fg, 52.25.Fi

Key Words: Ignition, Hohlraum, Non-LTE, High-Z ions, Electron-conduction

## Introduction

In late 2009, the National Ignition Campaign (NIC) team conducted the first experimental campaign of capsule implosions in ignition-scale gas-filled hohlraums using over 1 MJ of laser light at the National Ignition Facility (NIF). The goal of the campaign was to understand the energy balance in such a capsule/hohlraum/laser-pointing configuration. In general this campaign showed very good laser-hohlraum coupling [1], reasonably high drive [2], and good implosion symmetry control via the technique of cross beam transfer [3], to be discussed in further detail below. To date, based on extensive data analysis, all of these very positive conclusions remain essentially unchanged.

However, there were discrepancies between several types of data and the expectations based on (even post-shot) simulations using the standard simulation modeling methodology. In this paper we will describe the process whereby a new modeling methodology was introduced, called the “High Flux Model” (HFM). We will describe what it is, its historical antecedents, and its successes prior to this important campaign. We will explain why it predicts hohlraum plasma conditions different from the standard model, mainly a cooler electron temperature, and how this can explain most of the here-to-fore discrepant data. We will also stress that at the time of its application to this data set, it actually made one discrepancy between model and data even worse, and how resolving that issue demonstrated that the HFM was not only a “post-dictive” success, but also actually a correct predictor of important phenomenon.

In what follows, in Section 1 we will briefly review the data. Section 2 will list the discrepancies between data and the expectations based on the standard model. In

Section 3 we will describe the HFM. Section 4 will review the history of its development. In Section 5 we will summarize its application and successes in explaining the NIC 2009 data. So as not to interfere with the main flow of this narrative, we defer, to Appendix A, a discussion of the rather involved issues of electron conduction flux limiters and of non-local heat transport models.

### **Sec 1. The NIC Energetics Campaign of 2009**

The NIC 2009 energetics campaign progressed from sub MJ laser energies incident into smaller hohlraums, and culminated, on Dec. 4, 2009 when the NIF illuminated a full ignition scale cylindrical gold hohlraum, of length 1.0 cm and a diameter of 0.544 cm with over 1 MJ of laser light. At the hohlraum center was a 2 mm diameter capsule. The capsule was composed of a 180  $\mu\text{m}$  thick Ge-doped plastic shell filled with a (mostly He) gas that contained some deuterium to produce neutron signals. This capsule served as a surrogate to an ignition capsule that would have a frozen shell of equi-molar Deuterium / Tritium (DT) just inside the plastic shell. The hohlraum itself was filled with He gas in order to help hold back the expansion, into the interior of the hohlraum, of the portion of the gold walls heated to high (several keV) temperatures by the incident beams

The pulse shape was a typical ignition “shaped pulse” [4], namely a series of 3 pickets (that produce 3 shocks) followed by a main pulse between 16 and 19 ns which provides most of the drive. The NIF laser has 1/3 of its beams entering the vertical hohlraum (equally split to enter the top and bottom laser entrance holes (LEHs)) at 50° with respect to the hohlraum’s vertical rotational axis. Another 1/3 enter at 44.5°. These

two sets of beams, comprising 2/3 of the NIF power and energy are called “outer beams” because they intersect the walls of the hohlraum at an axial position roughly midway between the hohlraum waist and the LEH end-caps. The remaining 1/3 of the NIF beams are split equally between 30° and 23.5° beams that are called “inner beams” because they intersect the hohlraum wall at an axial position very near its waist, directly above the capsule situated at the hohlraum center. The NIF beams come in a cluster of 4 unit called a “quad”, with 32 outer quads and 16 inner quads.

The NIF was designed with the flexibility to change the “colors” of the laser beams in anticipation of the possibility that these color differences (“ $\Delta\lambda$ ”) could help control the transfer of energy between beams. When the beams overlap near the LEH, the local velocity field can provide a resonance which can facilitate Brillouin side scattering processes that transfer the energy from one beam to another [5].

This 2009 NIC gas-filled /capsule-imploding hohlraum energetics campaign showed good laser-hohlraum coupling [1]. Nearly 90% of the incident laser was absorbed by the hohlraum. That 90% level is high enough to mitigate stress on the laser system and help it to routinely provide sufficient incident power needed for ignition. The ~10% loss is due to scattered light produced by laser plasma instabilities (LPI). These include the Brillouin process in which the incident laser light stimulates ion waves, which then act as a grating/mirror to scatter that incident light (“SBS”). In a similar way the Raman process stimulates electron plasma waves that scatter the light (“SRS”). The scattered light’s power level and spectrum vs. time was measured on one 50° outer beam quad and on one 30° inner beam quad. In general the loss was due to SRS on the inner beams.

In addition, the SRS induced plasma waves eventually “break” and can accelerate electrons to high energy. These “hot-electrons” can pre-heat the capsule, making ignition more difficult. The hot electron temperature (“ $T_{\text{hot-e}}$ ”) and level (“ $f_{\text{hot-e}}$ ”) of hot electrons produced are inferred by the hard x-ray bremsstrahlung created as the hot electrons stop in the gold wall of the hohlraum.

The campaign also showed reasonably high drive [2] of nearly 300 eV. This is measured by a multi-broad-band-channel x-ray detector (with a coverage of 0.1-several keV photons) looking into the hohlraum through the LEH at an angle of  $37.5^\circ$ . The “brightness temperature” is determined by the observed x-ray power (integrated over the entire spectrum of emission), assuming (for the sake of definiteness) its emission area is the original LEH area. Of course the LEH is heated and closes in time. We post-process our simulations (that include that effect) and mimic the detector. Thus, we actually compare the radiant intensity (W/Sr) emitted from the hohlraum at the given viewing angle. The peak in time of this signal comes at 19 ns, at the end of the main drive pulse. Since the spectrum is close to a sub-keV Planckian in shape, the color temperature and brightness temperatures are quite similar. There is also a harder component, 1-3 keV, which is the “M-band” from the laser-heated gold that is also monitored. It too can preheat the fusion capsule, and the Ge doping of the plastic ablator shell is adjusted to mitigate this issue. The 300 eV level of radiation drive temperature is that required to implode the ignition capsule to sufficiently high velocity such that, upon stagnation, the hot spot temperature will be high enough for ignition [6].

The capsule implosion symmetry is another important parameter. Hohlräume naturally control short wavelength drive asymmetries just due to geometric, “view factor”

considerations [6,7]. However long wavelength (“P2” and “P4”) asymmetries are controlled by beam placement along the hohlraum walls and the relative power in the inner and outer beams. The outer beams make hot-spots on the hohlraum wall whose x-rays tend to push on the poles of the capsule, aligned with the vertical hohlraum axis. The inner beams counteract that push, by creating a hot source near the waist of the capsule, since they propagate to the wall at the waist of the hohlraum. The NIC 2009 campaign showed that we can control symmetry via cross beam transfer [3]. The implosions converged about a factor of 10 and their symmetry was monitored by measuring the shape of their  $\sim 5$  keV x-ray emission upon stagnation [1]. The images clearly went from severely “pancaked”, implying ineffective inner beam drive, to round as  $\Delta\lambda$  was increased, and power was transferred from outer to inner beams. Another metric of the increase of cross beam transfer from outer to inner beams as  $\Delta\lambda$  was increased, was the decrease in x-ray brightness of the spots at the positions where the outer beams hit the hohlraum wall. After optimizing, via this  $\Delta\lambda$  tool, the images were within about 10% of round, (from a P2 and P4 perspective) implying of order 1% (time integrated) drive symmetry. Actual ignition capsules will converge further, but we have yet to do a full campaign that monitors symmetry (and adjusts beam powers) in a time dependent way in order to ensure even better time-integrated symmetry. Nonetheless, these initial results are encouraging as they show that the  $\Delta\lambda$  technique acts in a reproducible and controllable way to transfer energy between beams to help achieve good symmetry.

While all of these results are very positive and very promising with regards to achieving hohlraum conditions conducive to driving targets to ignition, there were, however, a number of unresolved questions that remained. Achieving a fuller

understanding of the plasma conditions in the hohlraum and arriving at a more fully self consistent picture of the physics at play here, could lead to an even more optimized hohlraum. We discuss those discrepancies in detail, in the next section.

## **Sec 2. Discrepancies between the data and the simulation model's expectations**

Our expectations from any given shot during the campaign are formed by the following procedure. We use the radiation-hydrodynamic two-dimensional simulation code LASNEX [8]. We input the measured laser power but subtract from it the estimated SRS and SBS losses. The estimate takes the measured value of SBS and SRS detected on a single 50° outer beam quad, assumes this loss happens for all of the outer beam quads equally, and thus multiplies that observed value by 32. Similarly the losses measured on the single 30° inner beam quad are multiplied by 16.

One of the key ingredients of the simulation model is the choice of non-local-thermodynamic-equilibrium (NLTE) atomic physics model. Our standard model uses the XSN package [9]. It has done so for several decades based on analysis of gold disk emission data [10]. A second key ingredient is the choice of electron thermal flux limiter, which we will discuss in detail below. It was chosen to be  $f = 0.05$ , again based on that same Au disk data analysis [10]. In general, hohlraum data prior to NIF have been matched rather well by using this standard model [11].

For each experiment there was a conscious choice of the  $\Delta\lambda$  between inner and outer beams. The procedure by which we predict how much transfer of power occurs from outer to inner beams is described in detail elsewhere [12]. With all of these

ingredients, the simulation is performed and then post processed to mimic the diagnostics that report the data from the shot.

There were, in fact, a number of unresolved questions that arose when comparing the data from this campaign to our expectations based on the methodology described above:

- Why was the level of the Stimulated Raman Scatter (SRS) light, detected as it leaves the hohlraum, higher than expected?
- Why was its spectrum below 580 nm, when 650 nm was expected?
- Despite the incontrovertible fact that transfer of power took place from the outer to the inner beams as  $\Delta\lambda$  was increased, and, that SRS was coming from the inner beams, why did the SRS level not go up with  $\Delta\lambda$ ?
- Why did the hot electron fraction,  $f_{\text{hot-e}}$ , inferred from the hard x-rays, *not* track the SRS levels?
- Why did  $T_{\text{drive}}$  go down with  $\Delta\lambda$ ?
- Why was the slope of the hard x-ray spectrum,  $T_{\text{hot-e}}$ , 30 keV, when, based on the (surprising) SRS spectra we would expect 18 keV?
- Why was the drive of the September '09 shots more than predictions, and those of the Nov. '09 shots less than predictions? And finally,
- Why was the implosion, before applying the " $\Delta\lambda$  technique", pancaked, when it was designed (of course) to be round?

Other questions regarding capsule performance, yield, peak x-ray brightness times, hydro-dynamic instabilities, etc. are beyond the scope of this discussion, as they were, indeed, beyond the original scope of this energetics campaign. What would prove key in

unlocking the mystery of these discrepancies would be a better physics model. That is described in the next section.

### **Sec 3. The High Flux Model**

In the Spring of 2010, we deployed a hohlraum simulation model that has several improvements over that of the standard model, including a more complete atomic physics description. We call it the “high flux model” (HFM), because, when compared to the standard model, it produces a higher flux of x-ray emission and of electron heat from a given laser heated high-Z (such as Au) plasma.

The HFM uses a detailed configuration accounting (DCA) NLTE atomic physics package [13] with many tens of levels while accounting for tens of iso-electronic ionization states. The levels and transitions considered include  $\Delta n=0$  transitions, and dielectronic/auto-ionizing processes. This is in contradistinction to the standard model’s use of an XSN, 10 level, average atom NLTE model, which does not allow for  $\Delta n=0$  transitions, and which, in its default mode of operation, does not include dielectronic processes. (The XSN model does have an optional package that attempts to account for the dielectronic/autoionizing processes). We note the irony that the name "detailed configuration accounting" is somewhat of a misnomer here: the model used in hohlraum simulations is based on super-configurations described by principal quantum numbers and is considered to be highly averaged, except when compared to XSN. The reader is referred to Ref. [13] for the details of the implementation of this model. This paper will

focus on the application of this model to the important, ICF ignition relevant, problem at hand, namely the elucidation of the issues raised in the previous section.

The DCA model has been benchmarked extensively against even more detailed codes such as SCRAM [14]. For a given high Z ion, in a plasma at a fixed electron density and temperature, the DCA-predicted emissivity is greater than that predicted by the standard model. For example, [15], Au at a temperature T of 2 keV and a mass density  $\rho$  of 0.01 gm/cc has an emissivity of 7.4 TW/cc according to SCRAM, but only 3.1 TW/cc according to XSN. The DCA opinion is 7.9 TW/cc, quite close to SCRAM. In general, for a given hot, high Z plasma, the higher emissivity of DCA will more rapidly radiatively cool the plasma faster than the lower emissivity standard XSN model.

The second key element of the HFM is a more liberal electron heat flux limiter. Since this discussion is rather extensive, and can be a major detour from the flow of this narrative, we refer the reader to the details in Appendix A. In brief, a hot plasma with a steep temperature gradient violates the basic assumption of a local, Fick's law form of heat transport that is in the hydro codes. The basic assumption is that the heat-carrying electron's mean-free-path is short compare to the gradient length. Quite often it is decidedly not. To avoid non-physical results, the heat flux is limited to a fraction,  $f$ , of the free streaming heat flux,  $nvT$ , where  $n$  is the electron density and  $v$  is the thermal velocity. The HFM uses a relatively generous electron conduction flux limiter ( $f=0.15$ ), because that choice agrees favorably with the results obtained with a more physically motivated non-local transport model. That too is discussed in detail in the Appendix. The HFM thus has more conduction cooling when compared to the standard model's choice of a relatively more restrictive  $f=0.05$ .

The two key changes, DCA, and  $f=0.15$ , each contribute directly to radiatively and conductively cooling a hot plasma faster than the standard model. Moreover, in some sense the sum is greater than the parts. The cooler plasma due to more electron heat conduction places the ion in a somewhat cooler state with more electrons in “active” atomic levels, and thus they do more radiative cooling. Similarly, the dielectronic processes also accomplish that. Together, the DCA and the  $f=0.15$  re-inforce each other, and lead to a prediction of a hohlraum plasma that is substantially cooler than the standard simulation model. As shown explicitly in the figures in the Appendix the difference in  $T$  is  $\sim 4.5$  keV for the standard model vs.  $\sim 2.5$  keV in the HFM. This difference proved to be a key element in solving the “mysteries” discussed in Section 2. Before focusing on that solution, we first, for completeness, review the history of how this new model came to be.

#### **Sec 4. The history and development path of the High Flux Model**

The standard model was developed in the 1970s in an era of limited computer resources. [9,10], and was based on analysis of a laser heated gold disk’s emission from a small (relative to NIF) spot illuminated by a small amount of energy. While the XSN NLTE atomic physics model was ‘state of the art’ then, we were continually “on the lookout” for better models. In the mid 1980’s, in the context of laboratory x-ray laser research, [15], better models became available, albeit for low- $Z$  to mid- $Z$  elements, and mostly deployed in the “post-processing” mode, rather than as an in-line predictor of NLTE populations and emission. The importance of dielectronic recombination was certainly seen in that milieu. [16]. The DCA model continued to develop, and with more

powerful computers, it was eventually ready to be run “in-line” as an important component in the prediction of plasma conditions. A good example of this was in the Thomson scattering data that determined the T and the ionization stage of a laser heated Au disk. The data was matched well by an early version of DCA and was not matched by XSN [17].

Much effort by the NLTE community over the last decade has resulted in a better understanding of the most important aspects of modeling high-Z atomic systems. In particular, a series of workshops [18-22] produced results highlighting the importance of doubly-excited states and the critical role played by autoionization / dielectronic recombination. A key piece for inexpensively calculating this important process came from Chung et al [23], who showed that the simple formulation developed by Sobel'man et al [24] reproduces the results of detailed calculations very well. The improvements in the current version of DCA which pertain to hohlraum plasmas, followed from these advances.

Meanwhile, however, experiments continued to be analyzed via the standard model. Suter et al [14] pointed out that a key issue, as lasers and targets progressed upward in scale size, is the contribution of the volumetric laser heated Au coronal energy (and the emission there-from) to the general hohlraum energy balance. Whereas it was ~10% on Nova scale, ~ 20% on Omega scale [12], it exceeds 30% on NIF scale. While hohlraum energetics are generally dominated by wall loss, [6,7], which scales with hohlraum area, as we progress to larger scales the coronal terms can be important: Volume / Area ~ scale size. As such it is only of late, in the NIF era, that it was

absolutely crucial to accurately calculate (and measure) the coronal x-ray emission, and thus to truly need a detailed, full physics model such as DCA.

Quite analogous to the atomic physics issues are the electron transport issues. As discussed in the Appendix, there are numerous reasons why an effective flux limiter could be the restrictive value of 0.05. Many of those reasons involve finite spot effects, and the non-uniform 2 or even 3 dimensional issues of the cooler area and volume that surrounds the spot. Hohlräume such as those shot on Nova and Omega had their walls illuminated by tight laser spots. NIF's 192 large spot size beams more uniformly fill the hohlraum wall area. The uniformity may be a reason for the less restrictive, "classical" flux limiter of 0.15 being operative now.

In a closely related way, the Appendix also discusses in detail the Au spheres illuminated uniformly by the Omega laser at the University of Rochester's Laboratory for Laser Energetics (URLLE). These experiments, and their analysis [25, 26] are, in essence, the modern analog of the gold disk experiments of the 1970s [10]. Just as those old gold disks set the tone for the standard model, the Au spheres set the tone for the *new* model, namely the HFM. In particular, the spherical illumination uniformity in the Au sphere experiment may be the key ingredient in why the absorption and x-ray emission in those experiments are best matched with  $f=0.15$ . Again, in those experiments, the non-local electron transport package supports that  $f=0.15$  result (see Fig. A2 of the Appendix).

In addition, the DCA model applied to those experiments did a better job than XSN in reproducing the spectral shape of the emission. [26]. For example, for a 3 ns  $10^{14}\text{W/cm}^2$  illumination of the Au sphere, the observed spectrum [25] at the time of peak emission (just before the end of the 3 ns pulse) had 2 ~ equal height peaks of emission: A

~ 150 eV wide clump of emission centered around a photon energy of 350 and a ~ 300 eV wide clump of emission centered around a photon energy of 750 eV. The XSN prediction was a single dominant peak at ~ 750 eV, whereas the DCA model reproduced the data with 2 equal height peaks of the correct width and photon energy central positions.

In the lead-up to the NIF experiments, Suter et al [14] predicted that the NIF hohlraum's coronal emission (as calculated by DCA) will be so important (as a drive enhancer) that the NIF laser would need ~ 20% less incident laser power to achieve the required ignition-level drive, than the laser power needed as predicted by the standard model. This was based on some 1-Dimensional (1-D) spherically symmetric simulations. At ~ the same time, full 2-Dimensional simulations (2-D) [26] implied the savings would only be ~ 5% in the incident laser power requirements. In retrospect both of those calculations used only the "DCA half" of the HFM: both used an  $f=0.05$  flux limiter. Nonetheless this discrepancy in 1-D vs. 2-D predictions was puzzling at that time.

Then came NIF. The first experiments were empty hohlraums. The drive emitted from those hohlraums exceeded the standard model's prediction by ~ 25 to 30%! [27, 28]. In hindsight, had the full HFM (with  $f=0.15$ ) been deployed in the Suter et al 1-D pre-shot calculations, they would have predicted this high drive level almost exactly. The higher flux limit of the full HFM allows for greater absorption of the laser in this empty hohlraum, and even more coronal emission (as discussed above). Nonetheless, the essence of the prescient Suter et al prediction was there. The large coronal emission at NIF scale came to the fore, and blew the standard model out of the water.

On the basis of these empty hohlraum results, whose analysis now had the added realization of the importance of the  $f=0.15$  “other half” of the HFM, the full NIF gas-filled, capsule-containing ignition hohlraums were re-calculated. At a fixed laser power input, the HFM predicted a 10% higher drive than the standard model. Recall from just above, that the DCA-only “half of the HFM” gave a 5% enhancement; thus the  $f=0.15$  was supplying the other 5%. And yet, despite the evidence from the Au spheres and the NIF empty hohlraums, the HFM was not adopted for the full ignition hohlraums. Why was that? In part, in real time, we were not fully confident in the astounding drive results from the empty hohlraums. This was the first full NIF experimental campaign. There were large corrections to be made due to cable response. Caution was (quite properly) the byword. In addition, the  $\sim 10\%$  difference in drive predictions for the full ignition hohlraum seemed too small to abandon the standard model that had served us so well for decades. Also, it was deemed better to be “conservative” in our expectations of drive.

In addition there was still the unanswered question: Why was the original 1-D simulation prediction of 20% savings in NIF laser energy so much higher than the 2-D simulation’s prediction of 5%? (Or equivalently now, the full HFM’s 1-D prediction of 30% vs. the 2-D prediction of 10%?). We believe we can answer that question now, with the benefit of hindsight. A full 2-D simulation of an empty hohlraum has the hot laser-heated Au corona fill most of the volume in a semi-uniform way. Thus a uniform 1-D spherical simulation of that system is not too bad an approximation. Indeed the full 2-D simulations of the empty hohlraums do reproduce the 30% enhancement vs. the standard model [28]. The very same 2-D methodology applied to a gas-filled capsule-containing ignition hohlraum give a 10% enhancement of HFM over the standard model. Upon

inspection, the capsule blow-off and the gas-fill conspire to severely limit the laser heated Au coronal blow-off to a much smaller volume (than it had in the empty hohlraum). The volume is restricted both radially and especially axially: the inner beam absorption and the capsule blow-off severely restrict the size of the corona near the hohlraum waist. Thus, the 1-D hohlraum simulation with its large, uniform corona, was a rather poor approximation to this 2-D geometry with its much smaller corona. Therefore, the 1-D simulation with its overly large coronal emission produced an overly optimistic estimate of laser power savings for this gas-filled capsule-imploding ignition hohlraum geometry.

This concludes our narrative of the historical development of the HFM. It sat ready, willing and able to be applied to the 2009 NIC ignition hohlraum energetics campaign. Due to real time uncertainty in the astounding empty hohlraum data (which, in the end turned out to be true) and due to a desire to be conservative (at least with respect to drive expectations) the standard model was still the tool of choice going into the campaign. As we shall see in the next section, in hindsight, the choice of the standard model turned out to *not* be conservative with respect to LPI and coupling issues.

In the next section, the major one of this paper, we will describe how the HFM re-emerged to explain the discrepancies described in Section 2 above. As we shall see, despite the HFM's many past successes in correctly modeling high radiative fluxes seen in the Omega Laser Au sphere data [25, 26] and in explaining the surprisingly high drive seen in NIC empty-hohlraums [27, 28], it met some resistance when applied to the NIC 2009 campaign. In part, this was because it was initially thought that the HFM was over-predicting the drive in this 2009 energetics campaign. However, re-evaluating the total SRS losses (especially by properly interpreting the hot electron fraction) and by including

scattering losses in the later shots due to aging of the disposable debris shields (DDSs), brought the HFM drive predictions into agreement as well. Given that this improved model has led to an overall understanding of the hohlraum performance, by virtue of its consistency with a great variety of observations (described in detail below), the HFM has become the preferred hohlraum model for going forward towards ignition.

## **Sec 5. The HFM applied to the 2009 NIC hohlraum energetics campaign**

### **Sec 5.1 The Raman Spectrum and Levels**

The first breakthrough in explaining the discrepancies and inconsistencies that were delineated in Sec 2, came in a creative attempt to understand the observed SRS spectrum. In general, the gain of SRS will increase with both laser intensity  $I$  and electron density  $n$ , and it will decrease with  $T$ . The standard model predicted a rather high  $T$  in the fill gas that occupies most of the volume of the hohlraum. In particular, consider the “mid-point of the road” position, which is at about the midway point of the path of the inner laser beam as it moves from outside the hohlraum, through the LEH (the “beginning-of-the-road”) and eventually hits the hohlraum waist above the capsule (the “end-of-the-road”). In the standard model the “mid-point of the road” position was deemed too hot (it is  $\sim 4.4$  keV at a time near the end of laser peak power at  $\sim 19$  ns) to have much SRS gain there. The plasma is even hotter at the “beginning-of-the-road” near the LEH where the beams overlap. Also, at the LEH, the plasma is less dense since the plasma flows out of the hohlraum there, so on several counts the SRS was even less likely at the LEH. On the other hand, SRS was *most* likely near the cooler, denser region near the hohlraum waist, the “end-of-the-road” position.

As time progresses in the pulse, the density throughout the hohlraum rises, as does the plasma frequency. As such, the SRS scattered light shifts downward in frequency (upward in wavelength) throughout the pulse. The standard model thus predicted a spectral shift characteristic of the highest density (the high “end-of-the-road” density), and thus a large wavelength shift. That was not what was observed.

D. Hinkel and E. Williams et al [29] invoked two insights into getting theory to agree much better with the spectral data. One was to “fudge” and invoke an artificially lower T. This would allow SRS to happen at the “middle of the road” at a lower density. The second was to invoke a 3-dimensional effect. The nearest-neighbor inner-beams overlap in an azimuthal sense, and thus, are effectively more intense. They progress from complete overlap (3x the single beam intensity) at the LEH, to partial overlap (2x the single beam intensity at the “mid-point of the road” position) as they propagate, in an axial sense about halfway into the hohlraum. By the time they are at the hohlraum waist (the “end-of-the-road” position), the beams have all separated azimuthally. The combination of lower T and 2x the intensity at the “mid-point of the road” position now allows the peak SRS gain to occur there, at a lower density than previously thought, and thus to much better match the SRS spectrum vs. time.

Upon hearing of this result, we suggested [30] the use of the HFM, since it naturally gives an appropriately low  $T_e$  (due to its high radiative and electron flux cooling of the corona, as discussed above, in Sections 3 and 4) at that spatial point in the hohlraum (and at a density of about  $10^{21}$  electrons/cc). The HFM gives a T of about 2.6 keV, without the need for an artificial “fudge” of lowering T. The spectrum was thus matched “naturally”.

In addition, the HFM's cooler plasma leads to less Landau Damping and thus predicts, [29] higher levels of SRS (meaning, a higher fraction of incident energy back-reflected by SRS) than the standard model does with its hotter  $T_e$ . This higher level of SRS approximately agrees with observations, especially after SRS was re-evaluated to be even higher than initially believed, as will be discussed below.

## Sec 5.2 The Capsule Implosion Symmetry

Upon applying the HFM to the 2009 NIC hohlraum energetics campaign in support of the efforts to much better match the SRS spectrum, as described just above in Sec. 5.1, we discovered [30] a delightful bonus. We found that it was immediately clear that the HFM would match the observed implosion symmetry behavior. Relative to the standard model:

1. The outer beams, with their higher electron conduction, convert laser light to x-rays more efficiently. These x-rays shine on the poles of the capsule driving it towards a natural "pancaking" shape upon implosion.
2. The cooler plasma of the HFM inhibits (via inverse bremsstrahlung absorption) the propagation of the inner beams deeper into the hohlraum, thus preventing them from reaching the waist of the hohlraum wall surrounding the capsule waist. If they cannot reach there, they cannot provide the drive on the waist that they are supposed to supply which is needed to counter the outer beams' drive on the pole. They cannot efficiently produce a "sausaging - counter-force" to the outer beams "pancaking - force". A balance of forces would produce a round implosion. The standard model

with its hotter plasma produces such balance. The HFM with its cooler plasma inhibits the “sausaging” force, and results in an imbalance, a net “pancaking”. Thus, both effects, the enhanced outer beam drive, and the denial of the inner beams to getting to the hohlraum waist, both give a natural “pancaking” to an implosion, as observed. It takes cross-beam transfer (via  $\Delta\lambda$ ) to make the capsule implosion round, as observed. The detailed modeling of the symmetry vs  $\Delta\lambda$ , using the HFM, and its very successful matching of the data is discussed in detail in Ref [12] of R. Town, M. Rosen, et al.

Since most of the reportage to date involves symmetry vs.  $\Delta\lambda$ , [1, 3, 12] we present here an additional successful result of the HFM in its matching of symmetry data. Here we consider the change in implosion symmetry at fixed hohlraum and laser conditions, including, at a fixed  $\Delta\lambda$ . Instead, what is varied is the capsule’s CH ablator thickness: from the nominal 180  $\mu\text{m}$  to a thinner 155  $\mu\text{m}$ . The experiment went from round (a rather large  $\Delta\lambda$  was used in both shots) for the nominal case, to 40% P2 sausage for the thinner ablator.

The standard model (used here, incorrectly with no beam transfer (despite the high  $\Delta\lambda$  used in the experiment) in order to get the nominal case round) predicts a less than 20% P2 sausage for the thinner ablator. The HFM correctly gets the nominal capsule round (using a 65% enhancement of incident inner beam energy due to the transfer of energy from the outer beams to the inner beams, as is reasonable for the experimental value of  $\Delta\lambda$ ), and more significantly, gets the correct result for the thinner ablator: a +40% P2 sausage.

The physics of this difference is clear. The standard model's hot corona did not put much of a roadblock in front of the inner beam's propagation path to the wall at the hohlraum waist. So a thinner ablator, which fills the hohlraum with less plasma, simply made an "easy job easier". The HFM however, made life very difficult for the inner beams to propagate to the wall at the hohlraum waist. The thinner ablator put less plasma out into the hohlraum and thus made a "difficult job much easier". Hence the standard model predicted a very small change in the symmetry. The HFM predicted a very large change, and indeed it was that very large change that was observed.

### **Sec 5.3 Energy Balance**

Having succeeded in explaining the SRS spectrum and level, as well as the surprising pan-cake symmetry image (when little  $\Delta\lambda$  is applied) and the rapid sausageing of the symmetry image when the ablator thickness is diminished, it remained to be seen how well the HFM would explain the measured drive. For a given laser input (after subtracting off the measured losses, as per the procedure described in Sec. 2) the model should correctly match the observed drive if energy balance was intact.

The HFM immediately solved the prior (when using the standard model) discrepancy of too much drive for shots early in the campaign. The HFM, with its higher emissivity, naturally gives more drive than the standard model, for a given laser input. Early in the campaign the power was relatively low (compared to the MJ class experiments at the end of the campaign) so LPI coupling issues were small. In general, early in the campaign,  $\Delta\lambda$  tended to be small as well. The disposable debris shields were rather pristine early in the campaign as well. Thus the possible losses were accounted for.

In essence, the early-in-the-campaign high drive “discrepancy” was merely Mother Nature’s way of hinting to us that we should have been using the HFM, and not the less emissive standard model.

With the HFM now with the just described 5 triumphs (for those keeping score...) under its belt, the final and most important challenge was for it to demonstrate energy balance for the important MJ class shots late in the campaign. However, there was already a “missing energy” problem. Even with the low emitting standard model, the observed drive was lower than expectations (again, even with accounting for the known losses at that time). Applying the HFM to these shots, with its high emissivity, only made the “missing energy” problem worse! The observed drive was now much lower than (HFM based) expectations. It seemed as if the HFM had failed its most important test, since the 1 MJ shot was the culmination of the entire 2009 campaign, and the HFM made the drive discrepancy problem worse, not better!

It seemed to us highly unlikely that the HFM, a model with better physics than the standard model, a model that had been successful on previous data (Au spheres at Omega and empty NIC hohlraums), a model that had already explained 5 discrepancies in the 2009 NIC energetics data, could all of a sudden be so wrong. We then turned the problem on its head, and considered this challenge of “missing energy” to be an opportunity. It was an opportunity for the HFM to not only “post-dict” experimental data, but for it to boldly make a prediction. The prediction [30] had to be that there were more losses, and lower coupling to the hohlraum than had been assumed at that time (~ March 2010).

The prediction of more losses had several components. The first was rather obvious: that the disposable debris shields (DDSs) were aging by collecting debris, in

other words, doing their job! They had not been “disposed of” throughout the campaign, so it was quite plausible that, by late in the campaign, the built-up debris and damage sites might be scattering incident light into larger angles that would have some fraction of the incident light not enter the LEH in the first place. With the campaign over, these “veteran” DDSs were taken into a dedicated lab, and assessed. Indeed, they were deemed to be scattering  $\sim 5\%$  of the incident laser light into angles that would make it miss the LEH. [31]

The second component of the prediction was less obvious: that the level of the SRS losses was higher than presumed at the time. As the SRS level was only measured on the  $30^\circ$  inner beams, in order to restore energy balance for the HFM model via the route of postulating increased the level of losses, we were “forced” into the bold assertion / assumption that there was more SRS on the un-monitored  $23.5^\circ$  inner beams. In the previous sentence two phrases need commentary: by “more SRS”, we mean over and above the “going-in” (and reasonable) assumption that the SRS levels were the same on the un-monitored  $23.5^\circ$  beams, as they were on the measured  $30^\circ$  beams; by using the word “forced”, we mean it in the same sense of the famous dictum of Sherlock Holmes: “When you have eliminated the impossible, whatever remains, *however improbable*, must be the truth”. There was no good reason, at that time, for thinking that the  $23.5^\circ$  beams should behave differently than the  $30^\circ$  beams (in fact, to date, there still is none), so it was truly a bold prediction based solely on the necessity of energy balance (along with the assumption that the HFM is the  $\sim$  correct description of reality). It remained to be seen if this SRS prediction was true.

A breakthrough in confirming this prediction came when L. Divol and P. Michel et al [32] re-interpreted the hard x-ray spectrum, not in terms of a single (30 keV)  $T_{\text{hot-e}}$  and  $f_{\text{hot-e}}$ , but rather as a 2 temperature distribution:

1) A dominant  $f_{\text{warm}}$ , with an 18 keV  $T_{\text{warm}}$ . This is the value of  $T_{\text{warm}}$  that was expected from the observed (and now understood) SRS spectrum. The expectation is based on a  $T_{\text{warm}} \sim (1/2) m v_{\text{phase}}^2$  argument, where  $v_{\text{phase}}$  is the phase velocity of the plasma wave that both scatters the incident light out of the hohlraum and then breaks to create hot electrons.

2) A much smaller  $f_{\text{hotter}}$ , with a 60 keV  $T_{\text{hotter}}$ . This hotter component may be due to SRS happening at higher density (the “end-of-the-road” position above the capsule waist) whose reflected light would refract and be trapped within the hohlraum, or perhaps another LPI issue- the  $2\omega_p$  instability in which the laser light decays directly into 2 plasma waves.

Following through on this 2-temperature insight, they found that  $f_{\text{warm}}$  indeed increased as  $\Delta\lambda$  was raised. This made eminent sense, since more energy and power was “cross-beam-transferring” into the inner beams, where SRS was known to be happening, and the plasma wave of that SRS process produces hot electrons. Using the Manley Rowe relations, from that  $f_{\text{warm}}$  a total SRS can be inferred. Since we only observe SRS light from the  $30^\circ$  inner beams, subtracting that  $30^\circ$  data from the newly inferred total SRS tells us how much SRS is coming out of the  $23.5^\circ$  inner beams. What they found (from this long string of inferences) was that for the larger incident laser energy shots, with larger  $\Delta\lambda$  (such as the 1 MJ shot), there was indeed substantially more SRS on the  $23.5^\circ$  inner beams. In fact, there was as much as  $\sim 3x$  more energy scattered into the unmonitored

23.5<sup>0</sup> inner beams! These surprising results were completely in line with the SRS predictions “forced upon us” by the need for the HFM to conserve energy balance.

Theory [3] predicts that, as  $\Delta\lambda$  is increased, outer beam energy is transferred to both cones of the inner beam. An area of active investigation is to understand why the 30<sup>0</sup> inner beams’ SRS signal mysteriously stayed almost constant vs.  $\Delta\lambda$ , (as was observed in the NIC ’09 campaign), while the 23.5<sup>0</sup> beams’ SRS signal increased with  $\Delta\lambda$ , as was inferred by the data analysis method just described above. Massive plasma simulations are underway that could lead to some understanding of this phenomenon of a dichotomy between the two “flavors” of inner beams [29].

In summary, late in the campaign, as higher laser powers and higher values of  $\Delta\lambda$  were used (which, as described above, led to SRS in the un-monitored 23.5<sup>0</sup> beams), losses were larger. Those losses, as well as the DDS losses, were initially un-accounted for. Therefore, initially, the drive predictions were above the drive data for the Nov.-Dec. ’09 shots. Now, with all the losses accounted for, the HFM matches the observed radiant intensity emerging from the hohlraum. Again, as with the symmetry, R. Town, M. Rosen et al describe this agreement of the HFM drive with the data in great detail in Ref. [12].

Thus, the HFM had made some bold predictions, which appear to have come true. In addition, in this context of the Michel, Divol et al [32] work, we can now also explain the single remaining discrepancy on the long list of Section 2, namely the observed drop in  $T_{\text{drive}}$  with  $\Delta\lambda$ . The total SRS increased with  $\Delta\lambda$ , but, as we now believe, it was lost from the hohlraum by exiting the hohlraum in the unmonitored 23.5<sup>0</sup> inner beam lines. Thus, with more losses, the  $T_{\text{drive}}$  naturally drops. This too is documented in detail in R. Town, M. Rosen et al [12] which shows the HFM’s quantitative agreement with that data.

There was one question remaining. The total SRS loss, and the extra SRS loss occurring in the unmonitored  $23.5^0$  inner beams, as just discussed, was all based on a string of inferences from the hard x-ray spectrum. It would be far more convincing to actually measure the SRS on the  $23.5^0$  inner beams. Thus, the credibility of the HFM hung in the balance for nearly half a year as a diagnostic was prepared for a  $23.5^0$  inner beam line to do exactly that. What if this entire “house of cards” collapsed under an observation of SRS in that previously unmonitored beam line that would be different than the inferred amounts described above? As it turned out [12], in late 2010 the measurement was made, and the SRS levels directly observed agreed well with the SRS amounts that previously were only inferred, as described above. The HFM model had withstood the test.

## **Sec 6. Summary: Lessons learned and taken into the future**

Let us remember, that after all of this analysis, while the initially believed SRS loss level has now been re-evaluated as higher, we have *not* changed the drive assessment. The HFM supplies extra drive, and it matches the drive data while accounting for the extra losses. We have also *not* changed the level of hot electrons, just its detailed interpretation.

Reaching this understanding of the ignition scale hohlraums, based on finding consistency with the wide variety of data from the NIC '09 energetics campaign, has allowed us to project into the future and to invent new schemes for achieving even more optimal hohlraum conditions.

For example, incorporating a suggestion by E. Moses, P. Michel [32] has calculated a  $\Delta\lambda_{30-23.5}$  that transfers laser power from the  $23.5^0$  inner beams, which have proven to be more prone to SRS, to the more benign  $30^0$  inner beams. This is a possible method of reducing SRS losses (and reducing the level of hot electrons that they create) as we progress to the 1.3 MJ class ignition experiments. This experiment has actually been done, and the proof of principle been demonstrated. [33].

Another example of lessons learned taken into the future is the following. One of us (D. Callahan) has made HFM based design changes to hohlraum geometry. A somewhat shorter and somewhat wider hohlraum allows the inner beams better access to the waist. This minimizes the need for beam transfer in order to get round implosions. Less beam transfer to the inner beams can mitigate the SRS levels, as they will have less power in them, under this new design, than they had in the NIC 2009 campaign.

Another implication of the HFM is in moving forward to higher incident laser energies. The relatively lower T of the hohlraum plasma, as predicted by the HFM led to more SRS. A higher laser energy will heat up that plasma and lower the SRS gain. Indications that this has indeed occurred has been seen in the 2010 1.3 MJ shots. These too are described in somewhat more detail in Ref [12] of R. Town, M. Rosen et al.

## **Acknowledgements**

We are very grateful to the very large team of our colleagues who were responsible for the successful 2009 NIC hohlraum energetics campaign. Of particular note we wish to thank N. Meezan, principal designer, and S. Glenzer principal experimentalist. The parallel efforts in, and results from, the three-dimensional design

code, Hydra are also to be recognized, in particular the efforts of M. Marinak, M. Patel, and G. Kerbel. The collaborative efforts of S. Hansen and P. Springer in launching a renewed NLTE modeling initiative are greatly appreciated. We thank J. Lindl, J. Edwards, N. Landen, B. MacGowan, J. Atherton, J. Nuckolls, and E. Moses, as well as D. Pilkington, C. Verdon, and B. Goodwin, for their support and encouragement.

This work was performed by LLNL for the DoE under contract #DE-AC52-07NA27344.

## **Appendix A: The role of the “flux limiter” in modeling ICF targets**

### **A.1 Introduction:**

When a laser passes through a plasma, it is absorbed “classically” by inverse bremsstrahlung. The electric field (“E”) of the laser drives a free electron into oscillatory motion. When that electron suffers a collision, that reversible oscillatory energy becomes irreversible electron heating. The thermal energy thus produced is transferred to other parts of the plasma via electron heat conduction, which will then govern the spatial distribution of the electron temperature,  $T$ .

For systems in which the mean free path,  $\lambda$ , of the heat carrying electrons is much shorter than the electron temperature gradient scale length,  $L$ , a well defined expansion in the small parameter  $\lambda/L$  can be carried out, resulting in a first order result that the heat flux,  $F_e$ , down that  $T$  gradient can be described (in 1-D notation for now, for simplicity) as  $-\kappa_e dT/dx$ .

Unfortunately for many an ICF application, the situation is not so simple. Steep gradients and long mean free paths can make the expansion invalid. If we allowed the heat flux to be described *solely* as  $F_e = -\kappa_e dT/dx$ , absurd results could ensue, whereby the heat flux can exceed a physical limit of free streaming heat flux,  $n v T$ , where  $n$  is the electron density, and  $v$  is the thermal velocity. To ensure “non-absurdity” we typically make sure the flux does not exceed this limit, and for generality, impose a coefficient,  $f_L$ , “the flux limiter” on this term, resulting in “ $f_L n v T$ ”. The heat flux in a hydro code is then computed either as:

$$F_e = \min (-\kappa_e dT/dx, f_L n v T),$$

or, in a numerically smoother, “harmonic mean” formulation:

$$F_e = [(-\kappa_e dT/dx)^{-1} + (f_L n v T)^{-1}]^{-1}.$$

## A.2 Choosing a value for “ $f_L$ ”:

The central question is: What value of “ $f_L$ ” should we choose? A heuristic calculation, presented in the Atzeni & Meyer-ter-Vehn textbook [A1] (pg. 199) gives a value in the neighborhood of 0.1. The calculation follows from the classical, derivation of  $F_e$ , using an expansion in the small parameter  $\lambda/L$ . It treats the electron distribution function as a zero order Maxwellian (with temperature  $T$ ),  $f_{0M}$ , plus a first order term,  $\mu f_1(v)$ . Here  $\mu$  is the cosine of the angle between the temperature gradient,  $dT/dx$ , and the velocity vector. This  $f_1$  term carries the heat. The heat flux moment is calculated as an integral of  $(\mu v)(m v^2) \mu f_1(v,t) 2\pi v^2 dv d\mu$ . The resulting integrand is not monotonic in  $v$ . For values of  $y = (v/v_{th}) < 8^{1/2}$ , (with  $v = (kT/m)^{1/2}$ ), the integrand is actually negative. In other words, electrons with these velocities represent heat that is actually flowing up the

T gradient! This is the return current needed to ensure charge neutrality. For values of  $y = (v/v_{th}) > 8^{1/2}$ , the integrand is positive, representing net, “usual” heat conduction down the T gradient, wherein the heat is carried by the longer mean free path electrons. The value at which the integrand peaks,  $y=3.7$ , tells us the “typical” electron velocity that carries the heat. To ensure a “physical” result when the small parameter approximation begins to break down, we impose the heuristic requirement that  $f_L$ , evaluated at  $y=3.7$ , not exceed  $f_{0M}$ . This requirement leads to an equivalent requirement that the resultant heat flux not exceed  $(0.1) nvT$ , in other words, a value of “ $f_L$ ” of 0.1.

Of course the actual answer will be far more complicated and depend on the exact convolutions / velocity integration. As an example, consider the results of a calculation performed by the URLLE [A2]. Here, a Fokker Planck code is run for a typical direct drive implosion, resulting in a value for the heat conduction. A hydro-code is run, and “ $f_L(t)$ ” is varied in time in such a way that the hydro code matches that Fokker Planck result for each time. This procedure results in an  $f_L$  that varies in time between 0.12 and 0.06, in the neighborhood of the heuristic derivation described above. More importantly, we note the general complexity of the problem. Even for this simplified application, there is no single “correct” value for  $f_L$ . It varies in time, and varies in range between a typical “high flux” value of 0.12 and an inhibited “low flux” value of 0.06.

It is really no surprise that there is no single “correct” value for  $f_L$ . Especially in physical situations in which phenomena occur that are not accurately treated in the hydro codes, heat conduction can behave as if it is effectively “inhibited”. To match the data from such systems, values of  $f_L$  such as 0.03 - 0.05 have often been used. Examples of such underlying, un-modeled physics could be “sub grid” ion acoustic turbulence that

effectively acts as increased collisionality to long mean free path heat carrying electrons, Weibel instabilities that lead to “sub grid” but strong B fields that may inhibit cross-field transport, and larger scale MHD generated B fields that also can inhibit the high velocity, long mean free path heat carrying electrons. This latter effect can in principle be modeled explicitly (it is *not* “sub grid”). However, owing to the many complicated MHD terms that can generate B fields, great computational care and cost is involved in correctly including them explicitly in 2-D. The fact that MHD effects are inherently 3-D, complicate the issue even further. As a result, such calculations are not currently tractable. In addition, high power laser absorption in high Z plasmas often leads to the “Langdon effect” [A3] which produces non-Maxwellian electron population distributions which complicate things even further still!

Having become inured to such low values of  $f_L$  (for all of the possible reasons just discussed) over many years and many experiments, we were somewhat surprised when modeling the x-ray emission from Au coated spheres [25] on the Omega laser at the URLLE. The usual low value of  $f_L$  (= 0.05) led to too high a coronal T, because energy is not transported deeper into the target, so it is bottled up in the under-dense corona and heats it to high values. This high T led to too low a collisionality and thus too low an absorption fraction of the laser. Moreover, the low, inhibited flux limit led to too low an efficiency of converting absorbed laser into x-rays because too little energy is transported deeper into the target where denser warm material is the “sweet spot” for making x-rays. All told, the resulting prediction of the x-rays emitted by these Au spheres was low by a factor of two. The data was fit much better by a value of  $f_L$  of 0.15.

A possible reason for this “classical” behavior is the removal of flux inhibiting transverse gradients in this spherically symmetric situation (as well as possible radiative smoothing of non-uniformities in the corona). When applied to the large plasmas and large spot-size laser beams of a NIF hohlraum, it is possible that similar arguments could be applied, and thus at least a plausible expectation that for NIF hohlraums a high value of  $f_L$  could be in play. Thus using  $f_L = 0.15$  in the “High Flux Model” that seems to correctly describe the plasma conditions and a great deal of the NIC data is not that unreasonable. Further support for this value came from comparisons with non-local models, to be discussed next.

### A.3 Non-local Models

Given the inherent non-local nature of long mean-free-path large-velocity heat-flow-carrying electrons transporting energy large distances across locally steep  $T$  gradients, there is a clear need to incorporate that more relevant physics into the hydro codes, and thus to replace the fundamentally flawed approach of a local description of heat flow and the “ $f_L$ ” crutch upon which it stands. There are many different non-local models that have been incorporated into 1-D and into 2-D hydro codes. We will briefly mention a few.

The Luciani, Mora, and Virmont model [A4] finds  $F_e(x)$  as a convolution:

$$\int F_e(x')G(x,x')dx'$$

The non-local propagator is given by:

$$G(x,x') = \frac{\exp\left\{-\int_{x'}^x \frac{dx''}{\lambda(x'')}\right\}}{2\lambda(x')}$$

This is usually run in 1-D. As it is explicitly non-local and couples every zone to every other zone, it scales rather unfavorably in big 2-D runs. The Schurtz, Nicolai and Busquet [A5] model uses a Krook collision operator and a multi-group electron approach, which scales much better for the big 2-D runs. The Manheimer, Colombant, and Goncharov model(s) [A6] also use a Krook operator but treat the E field / return current correction differently. All of these models have had some degree of validity established by comparisons with Fokker Planck treatments in various test problems. Recent work by A. Prochaska and G. Moses [A7] shows a favorable comparison of the Schurtz et al and the Manheimer et al models.

The Schurtz et al non-local model was implemented in the 3-D radiation hydrodynamics code Hydra [A8]. Based on promising results [A9] seen there, it was then implemented into Lasnex. It is the Lasnex results and comparisons that we show next. In Fig. (A1) below we show the change (going clockwise from the upper left) in plasma conditions (at a fixed time of 18 ns, midway through the main pulse) of an ignition hohlraum in 2 steps from the standard model to the High Flux model. The temperature contour color-scale (0 to 5 keV) is the same for every one of the 4 panels. The y-axis is the radial direction, from 0 to 0.4 cm, of the cylindrical hohlraum. The x-axis is the axis of rotation, from 0. to 0.55 cm. The simulation extends even further along that axis. Thus the “right half” of the hohlraum is simulated, with mirror symmetry assumed. While, by convention, the rotation axis is “horizontal” here, in NIF it is vertical. The radiatively driven capsule at the center is “blacked out” to avoid distraction.

The upper left panel of Fig. (A1) is the XSN  $f=0.05$  model and shows a very hot hohlraum plasma (for a “mid-point on the road” SRS relevant location, at  $R=0.2$ ,  $Z=0.2$ )

of about  $T = 4.5$  keV. The upper right is the DCA model with  $f=0.05$  and shows a cooler hohlraum plasma: at the same reference location its  $T$  value is about 3.3 keV. The lower right is the full HFM (DCA and  $f=0.15$ ) and it is cooler yet, with  $T$  about 2.5 keV. The final comparison (lower right to lower left) is the  $f_L=0.15$  to the non – local model.

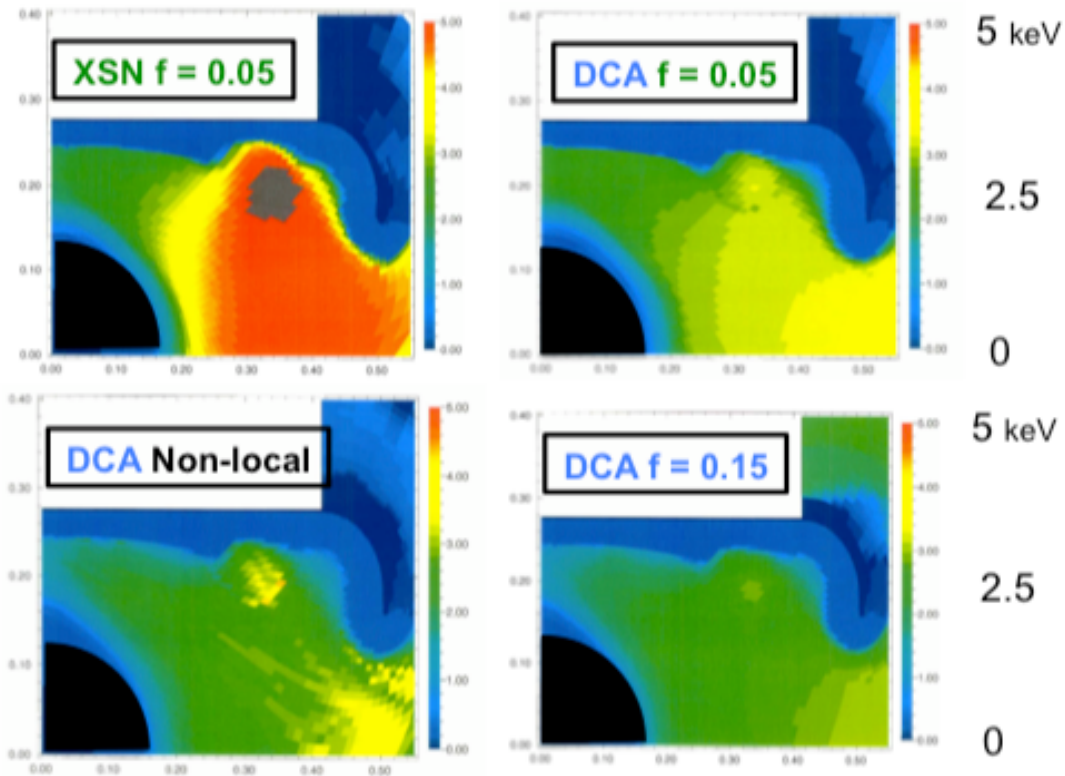


Figure (A1): Comparison of 2-D hohlraums' plasma electron temperature for 4 different models at a time  $t=18$  ns (the middle of the main pulse).

For locations well within the volume of the hohlraum (say,  $R=0.2$ ,  $Z=0.2$ ) it is clear from the figure that the non-local and the  $f_L=0.15$  agree best, with both having a  $T$  of about 2.5

keV. At these locations important laser plasma interactions such as Raman scattering may take place. At the laser entrance hole the figure does show some differences between the two models, which do need to be taken into account when calculating the cross-beam transfer that may occur there.

This general behavior can also be seen in 1-D simulations of the URLLE experiments on Au coated spheres. In Fig (A2) we show T profiles at a time of 0.9 ns, 0.1 ns before the end of the 1 ns  $10^{15}$  W/cm<sup>2</sup> irradiation. The y-axis goes from 0 to 5 keV, and the x-axis is the radial direction, and goes from 0.04 to 0.09 cm. The original radius of the Au sphere was at 0.04839 cm. In decreasing values of peak T they are: XSN,  $f=0.05$  (green / dot-dash); DCA,  $f=0.05$  (green dotted); DCA,  $f=0.15$  (red / dashed); and DCA non-local electron transport (black). The values of T are quite close, in each model, to that at the center of the 2-D hohlraum calculation of Fig. (A1). Again we see the close agreement between the  $f=0.15$  and the non-local electron transport result.

What can certainly be said of this set of 1-D calculations is that each run is well resolved and numerically converged. Each run uses 400 radial zones to model the very thin ( $\sim 1\mu\text{m}$ ) layer of Au that is heated by the laser. At any given time throughout the pulse there is the challenging ultra-thin region just within the critical density radius. Proceeding in the inward radial direction, the rapidly dropping T, and rapidly rising density create a ‘sweet spot’ for the radial layer that best converts thermal energy to radiation. In these runs that ultra-thin conversion layer has  $\sim 10$  zones which is sufficient to be well resolved and numerically converged.

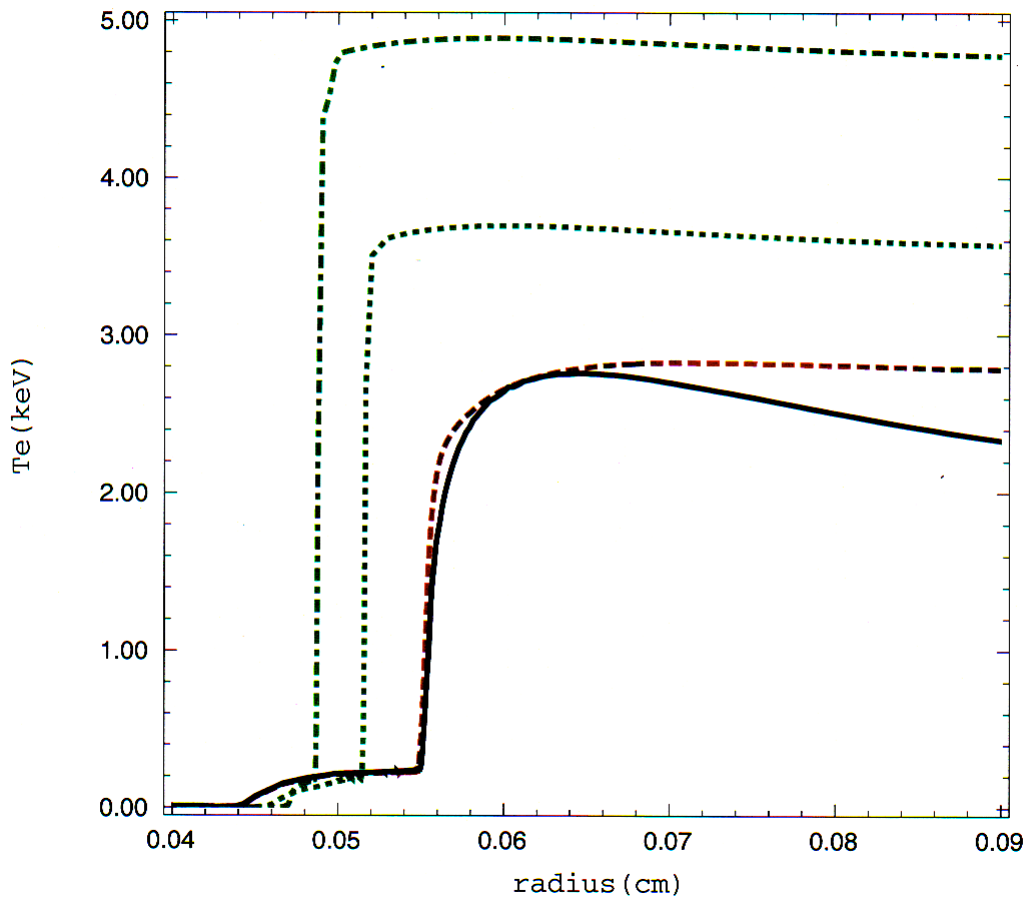


Figure (A2): Comparison of T profiles on a 1-D Au sphere for 4 different models

#### A.4 Summary:

With the advent of non-local electron transport models in 2-D simulations, the use of a flux limiter may soon go the way of the horse and buggy. The complexities of properly modeling high Z hohlraums still remain a challenge. Besides “sub-grid” physics issues, electron population distribution functions may be inherently non-Maxwellian, which can affect the radiation physics, which in turn can affect the distribution functions,

as well as the gross plasma conditions. As always, we do the best we can with the tools we have, and keep our eye on better methodologies that advanced computer capabilities may allow us to implement in the future.

### References:

1. S. H. Glenzer, B. J. MacGowan, P. Michel, et al, *Science* **327**, 1228 (2010).
2. N. B. Meezan, L. J. Atherton, D. A. Callahan, et al *Phys of Plasmas* **17**, 056304 (2010)
3. P. Michel , S. H. Glenzer, L. Divol, et al, *Phys of Plasmas* **17**, 056305 (2010)
4. S. W. Haan, J. D. Lindl, D. A. Callahan, et al, to appear in *Phys of Plasmas* **18** (2011)
5. P. Michel, L. Divol, E. A. Williams et al, *Phys. Rev. Lett.* **102**, 025004 (2009).
6. M. D. Rosen, *Phys of Plasmas* **6**, 1690 (1999)
7. Mordecai D. Rosen, “Fundamentals of ICF Hohlräume”, in “Lectures in the Scottish Universities Summer School in Physics, 2005, on High Energy Laser Matter Interactions”, D. A. Jaroszynski, R. Bingham, and R. A. Cairns, editors, CRC Press Boca Raton. Pgs 325-353, (2009).
8. G. B. Zimmerman and W. L. Kruer , *Comm. Plasma Phys. Control. Fusion* **2**, 51 (1975)
9. See National Technical Information Service Document No. UCRL52276 (W. A. Lokke and W. H. Grasberger, Report No. UCRL-52276, 1977). Copies may be ordered from the National Technical Information Service, Springfield, VA.
10. M. D. Rosen, D. W. Phillion, V. C. Rupert, et al, *Phys. Fluids* **22**, 2020 (1979).
11. L. J. Suter, R. L. Kauffman, C. B. Darrow, et al, *Physics of Plasmas* **3**, 2057 (1996).
12. R. P. J. Town, M. D. Rosen, P. Michel, et al, to be published in *Physics of Plasmas* (2010).

13. H. Scott and S. Hansen, High Energy Density Physics 6, 39 (2010).
14. L. Suter, S. Hansen, M. D. Rosen, P. Springer, and S. Haan, in “Atomic processes in Plasmas 2009”, K. Fournier editor. American Institute of Physics IOP Publishers pgs 3-9, (2009).
15. M. D. Rosen, P. L. Hagelstein, D. L. Matthews, et. al, Phys. Rev. Lett. **54**, 106 (1985).
16. P. L. Hagelstein, M. D. Rosen, and V. L. Jacobs, Phys. Rev. A, **34**, 1931 (1986).
17. S. Glenzer, W. Rozmus, B. MacGowan, et al, Phys. Rev. Lett. **82**, 97 (1999).
18. R.W. Lee, J.K. Nash, Yu. Ralchenko, J. Quant. Spectrosc. Radiat. Transf. **58**, 131 (1997).
19. C. Bowen, A. Decoster, C.J. Fontes, et al, J. Quant. Spectrosc. Radiat. Transf. **81**, 71 (2003).
20. C. Bowen, R.W. Lee, Yu. Ralchenko, J. Quant. Spectrosc. Radiat. Transf. **99**, 102 (2006).
21. J. Rubiano, R. Florido, C. Bowen, et al, High Energy Density Phys. **3**, 225 (2007).
22. C.J. Fontes, J. Abdfallah Jr., C. Bowen, et al , High Energy Density Phys. **5**, 15 (2009).
23. H.-K. Chung, M.H. Chen, W.L. Morgan, et al, High Energy Density Phys. **1**, 3 (2005).
24. I.I. Sobel'man, L.A. Vainstein, E.A. Yukov, Excitation of Atoms and Broadening of Spectral Lines, second ed., Springer, Berlin, 1995.
25. E. L. Dewald, M. D. Rosen, S. Glenzer, et al, Phys. of Plasma **15**, 072706 (2008).
26. M. D. Rosen, H. A. Scott, L. J. Suter, and S. Hansen, B.A.P.S. 2008.DPP.BP6.28 (2008).
27. J. L. Kline, S. H. Glenzer , R. E. Olsen, et. al, Rev. Sci Instr. **81**, 10 10E321 Oct.(2010).
28. R. E. Olsen, L. J. Suter, J. L. Kline, D. A. Callahan, M. D. Rosen, et al, in “Inertial Fusion Sciences and Applications 2009”, B. Hammel, C. Laubanne, H. Azechi, editors. Journal of Physics, IOP Publishers (2009).
29. D. E. Hinkel, M. D. Rosen, E. A. Williams, et al, to be published in Physics of Plasmas (2010).
30. M. D. Rosen, Tech. Rep. LLNL-PRES-428527 3/18/10, LLNL (2010).
31. C. Haynam, et. al., LLNL, private communication, April 2010.

32. P. Michel, R. P. J. Town, L. Divol, M. D. Rosen et al, to be published in Phys. Rev. E (2010).
33. J. Moody et al, in preparation. (2010)
- A1. S. Atzeni and J. Meyer-ter-Vehn “The physics of inertial fusion”, pgs. 198 – 201, Clarendon Press, Oxford, (2004).
- A2. A. Sunahara, J. A. Delletrez, C. Stoeckl, et al Phys. Rev. Lett. **91**, 095003 (2003).
- A3. B. Langdon, Phys. Rev. Lett. **44**, 575 (1980)
- A4. X. Luciani, P. Mora, and J. Virmont Phys. Rev. Lett, **51**, 1664 (1983)
- A5. G. Schurtz, X. Nicolai and M. Busquet, Phys. of Plasma **7**, 4238 (2000)
- A6. W. Manheimer, D. Colombant , and V. Goncharov Phys. of Plasma **15**, 083103 (2008)
- A7. A. Prochaska and G. Moses, Bull. Am. Phys. Soc. **55**, No. 15, 230 (2010)
- A8. M. M. Marinak, G. D. Kerbel, N. A. Gentile, O. Jones, D. Munro, S. Pollaine, T. R. Dittrich, and S. W. Haan, [Phys. Plasmas](#) **8**, 2275, (2001).
- A9. R. A. London et al to be published.